

COMMISSARIAT A L'ENERGIE ATOMIQUE

CENTRE D'ETUDES NUCLEAIRES DE SACLAY

Service de Documentation

F91191 GIF SUR YVETTE CEDEX

CEA-CONF -- 9102

L3

CEA-SPhT--87-98

A MICROSCOPIC DESCRIPTION OF NUCLEAR SHAPES

Bonche, P. CEA CEN Saclay, 91-Gif-sur-Yvette (France). Service
de Physique Theorique

Communication présentée à : International conference on nuclear shapes
Aghia Pelagia (Greece)
28 Jun - 4 Jul 1987

A MICROSCOPIC DESCRIPTION OF NUCLEAR SHAPES

P. BONCHE

Service de Physique Théorique
CEN-Saclay
91191 Gif-sur-Yvette Cedex
FRANCE

ABSTRACT

This talk describes recent three-dimensional self-consistent Hartree-Fock calculations. After an introduction providing the basic approximations and the different symmetries, we present an application to quadrupole deformation. We pursue with a study of octupole deformation properties of ^{222}Ra and ^{144}Ba nuclei for which states of good (positive and negative) parity are projected out. Finally we discuss an extension to the study of rotation and high-spin states with the cranked self-consistent Hartree-Fock method. As an exemple, the ^{24}Mg nucleus is studied as a function of angular momentum from ground state up to fission.

The work presented below has been done in collaboration with H. Flocard and P.-H. Heenen.

International Conference on Nuclear Shapes
CREETE GREECE 28 June - 4 July 1987

Saclay PhT/87-98

INTRODUCTION.

The analysis of the behaviour of nuclei subject to various constraints provides a useful testing ground both for effective nuclear forces and for different theoretical descriptions ranging from phenomenological, such as the liquid drop, to fully microscopic, like Hartree-Fock. The following question still remains a challenge: assuming one knows the correct effective force, how much microscropy is needed in the description of the nuclei in order to describe accurately a given set of physical properties? Although effective forces are always somehow model dependant, this question remains relevant as most models have in common the physical picture of independant particle motion of each nucleon in the mean-field created by the average interaction with all the others. In this talk, we present a description of nuclear deformation properties by means of the microscopic self-consistent Hartree-Fock (H.F.) method which is presently the most successful of the available microscopic models.

In the H.F. approximation, contrary to Strutinsky-type potential-energy calculations [1] for instance, the potential shapes are not constrained a priori to conform to simple analytical shapes. As a result one avoids all the sometimes tedious work of optimization with respect to parameters of the mean-field potential, like β_5 or β_6 , considered as physically irrelevant. Furthermore, the nuclear energy is not split in bulk and microscopic contributions and the solution of the Hartree-Fock equations, with appropriate constraints, gives the total energy. In a single calculation it provides the single-particle wave functions and spectrum, as well as the optimal shape for the nucleus subject to the chosen constraints: quadrupole, octupole deformation or rotational frequency. By optimal shape, we mean that the energy is minimized with respect to variations of all unconstrained degrees of freedom (Y_4, Y_5, Y_6, \dots). An additional difference with Strutinsky-like calculations lies in the fact that the deformations are defined with respect to the intrinsic state rather than the potential and are therefore in closer contact with experimental information like that provided by electromagnetic transition.

As described above, the H.F. approach, when tractable, is a much better candidate to the description of nuclear properties than the presently used methods, which anyhow are in general established by introducing approximations on the Hartree-Fock model. There are however several technical limitations which render H.F. calculations difficult and time consuming. In the sixties and the early seventies, H.F. equations were solved by expanding the self-consistent single-particle wave function on a basis. This necessarily truncated basis introduced artificial constraints on either the shape of the nucleus or the asymptotic behaviour of the wave functions. To overcome this difficulty we have chosen to discretize the H.F. equations on a regular mesh in coordinate space [2]. The number of points of the mesh required for an accurate description of nuclei is rather large and constitutes the price one has to pay to avoid the limitation generated by the basis. This technological improvement is made possible by the present availability of large vectorized computers. An other difficulty arises with some proposed nuclear effective forces which produce non-local mean-field due to exchange terms in the interaction. With such forces, the computation time would be so large that calculations are not presently feasible. To circumvent this difficulty we use Skyrme-type forces which produce local mean-field and which, despite their simplicity, have turned out to be very successful. For completeness however, let us mention an alternate approach where the H.F.-Bogoliubov equations are solved in a basis with a two-body force which produces a non-local mean-field. The latter method of solution has not been used to study rotations yet, but rather to analyse extensively the fission properties of nuclei [3].

This talk is organized as follows. First we review the H.F. method in coordinate space with Skyrme forces and present some results for nuclei with quadrupole deformations. Then we discuss results for the octupole deformation of ^{222}Ra and ^{144}Ba nuclei. In these cases, a restoration of the broken parity is also performed by projection of the intrinsic state onto states with good parity. Finally we turn to the problem of the self-consistent cranked H.F. equations with a calculation of the ^{24}Mg Yrast line up to fission.

CONSTRAINED H.F. EQUATIONS IN COORDINATE SPACE

Let us first focus on time-reversal invariant intrinsic states with the Skyrme interaction. The H.F. energy can be written as the integral of a local hamiltonian density $\mathcal{H}(r)$:

$$E = \int \mathcal{H}(r) d^3r, \quad (1)$$

where $\mathcal{H}(r)$ depends on the single-particle wave functions through various local densities (kinetic energy, matter and spin densities) [2]. In our calculation, the direct term of the coulomb energy is treated exactly while we use the Slater approximation for the exchange one.

For nuclei which do not present odd multipolarity deformations, two additional symmetries can be imposed on the single-particle wave functions: the parity and the signature, the latter corresponding to a rotation of π around the z -axis. It is then possible to impose that each of the four components (real and imaginary part, spin up and down component) of each single-particle wave function has a given parity with respect to the three symmetry planes $x=0$, $y=0$ and $z=0$ (see ref [2] for a complete discussion). The H.F. equations derived from the variation of the energy (eq. 1) can then be solved in a rectangular box covering only one eighth of the full space.

As in this section we restrict our discussion to time-reversal invariant wave functions, the single-particle orbitals can also be arranged in time-reversed pairs Φ_i and $\Phi_{\bar{i}}$ such that

$$\Phi_{\bar{i}}(r, \sigma) = (\hat{T} \Phi_i)(r, \sigma) = \sigma \Phi_i^*(r, -\sigma), \quad (2)$$

where \hat{T} is the time-reversal operator, so that it is sufficient to solve the H.F. equations for only one member of the paired states. This provides an additional reduction of the computational task by a factor two.

Pairing correlations are included in an approximate manner within the BCS formalism using a simple seniority force. We use a

constant pairing strength G with cut-off factors f_i which prevent the unrealistic pairing of highly excited states of the continuum [2]. The pairing contribution to the energy reads as:

$$E_p = -G \sum_{i,j>0} f_i f_j (u_i v_i)(u_j v_j), \quad (3)$$

where the paired states are the two time-reversed orbitals Φ_i and Φ_i^- .

Deformation energy surfaces are obtained by means of an external constraint on the mass quadrupole tensor $Q_{ij} = (3x_i x_j - r^2 \delta_{ij})$ with adequate Lagrange multipliers. All other unconstrained degrees of freedom (hexadecapole, ...) are fully relaxed. The symmetries discussed above impose that the principal axes of inertia lie along the axes.

All the results presented below have been obtained with the Skyrme interaction SIII. This interaction has some deficiencies (mostly regarding its rather large modulus of incompressibility), but has been extensively tested over the whole mass table. At the present stage, none of the Skyrme parametrizations proposed to cure the SIII deficiencies does it without introducing other problems.

The first application of the discretized version of the H.F. approximation has been an extensive analysis of the Zr isotopes [2] from the proton rich ^{76}Zr toward the neutron drip line. Exotic isotopes of neighbouring nuclei (Sr, Kr and Mo) were also investigated. Our calculation reproduces the experimentally well established transitions from spherical to well-defined rotor. A comparison with earlier works [4-7] using the Strutinsky method shows a good average agreement. We find a triaxial stability of the deformed ground states in the $N \sim 38$ and $N \sim 60$ regions in good agreement with the observed trends.

Heavier nuclei have also been studied with a similar success. For instance, A. Coc has studied the possibility of triaxial shape in the Cs region [8], whereas N. Redon has calculated the ^{138}Sm , ^{192}Os and ^{186}Pt nuclei, also looking for triaxial stable deformations [9]. Proton-rich exotic nuclei recently discovered at SARA in the Sm region ($^{134,136}\text{Sm}$) have also been investigated by N. Redon et al. [10]. We will not elaborate on these works which are already published.

Let us only mention the recent study by F. Naulin [11] who has made a extensive analysis of the properties of the neutron-rich even isotopes of C, O, Ne and Mg nuclei. One of his findings is that it is possible to get for these lighth nuclei binding energies with an accuracy of the order of ± 0.75 Mev. This precision is comparable to that of semi-empirical mass formulae [12,13], and even better in some cases. Figure 1 shows a comparison of his H.F. calculations of the 2-neutrons separation energies S_{2n} with experimental numbers, when available, and with the predictions of Uno and Yamada [12] or of Möller *et al.* [13].

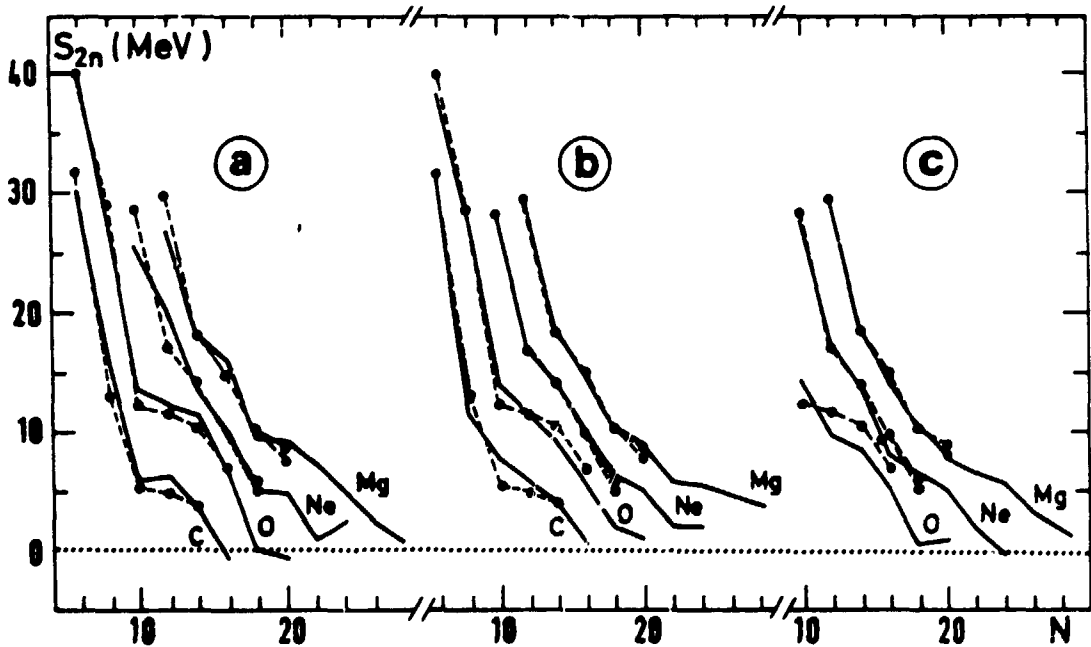


Fig. 1. Separation energies S_{2n} for different isotopes of C, O, Ne and Mg as a function of the neutron number N . a) H.F. calculations; b) Uno and Yamada mass formula [12]; c) Möller *et al.* [13] predictions. Experimental numbers are indicated by crosses, the solid lines join calculated values.

This result is quite interesting as these microscopic H.F. calculations are based on an effective two-body interaction involving

a very small number of parameters which are the same for all nuclei, contrary to semi-empirical formulae. The strength of the pairing force may need to be readjusted for different mass regions, however the results of Naulin have been obtained with the pairing strength used for the Zr region in ref. 2.

OCTUPOLE DEFORMATION.

Quasi-molecular rotational bands characterized by spin states of alternating parity connected by enhanced E1 transition [14] have been observed in several regions of the periodic table such as the barium [15,16] and the radium-thorium regions [15,17]. These bands can be understood by assuming that the corresponding nuclei have no intrinsic parity and that they have a pear-shape deformation in their ground states.

To explore the corresponding H.F. deformation energy surfaces, we include an additional constraint on the octupole moment $Q_3 = r^3 Y_{30}$ of the nucleus. The symmetry associated with the parity operator is broken by the Q_3 operator so that the single-particle wave functions keep only one good quantum number: the signature. As compared to the above calculations, it is necessary to double the size of the box by suppressing parity with respect to the $z=0$ plane, at the cost of a factor two increase in the computational task.

The first nucleus selected was the ^{222}Ra [18]. In view of the available data, it is not the best candidate for a study of permanent octupole deformation in the ground state. In fact, our choice was motivated by the discovery of the natural radioactive decay of this isotope by emission of ^{14}C [19]. Figure 2 summarizes our results. The symmetric ($Q_3=0$) minimum as a function of quadrupole deformation turns out to be a saddle point when both octupole and quadrupole degrees of freedom are introduced. The intrinsic state has an octupole moment of about 2000 fm^3 and a quadrupole moment 1310 fm^2 . This value of Q_2 is slightly larger than that at the saddle point (1020 fm^2). Since the intrinsic state breaks the reflection symmetry while the saddle point

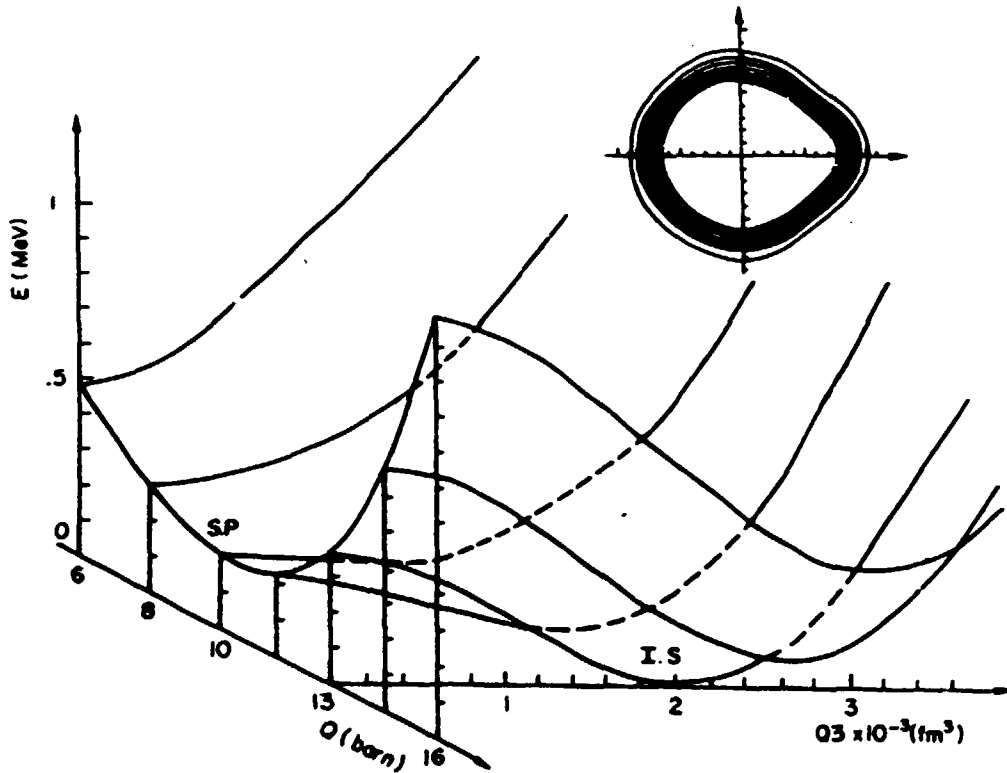


Fig. 2. Octupole deformation energy of ^{222}Ra for fixed values of Q_2 . The curves correspond to Q_2 (barn) = 6, 8, 11.5, 14.5 and 16. The contour lines (up-right corner) are drawn for the mass density of the intrinsic (I.S.) state with a density increase of 0.02 fm^3 between lines.

does not, one can expect that the band heads for both parities will have different quadrupole moments. To check this point, it is necessary to project H.F. wave functions onto good parity states. This requires going beyond the mean-field approximation and the calculation of matrix elements of the interaction between different H.F.+BCS states. We have developed a program for that purpose and used it for the ^{222}Ra . After projection, the energies and positions of the band heads of both parities are given in table 1. As expected, the negative parity state has a larger quadrupole moment. It should induce a larger moment of inertia for this band, in agreement with experimental

Table 1

Q_2	Q_3	E	E_+	E_-	
fm^2	fm^3	Mev	Mev	Mev	
1020	0	1703.33	1703.33	-	saddle point
1151	1010	1703.38	1704.06	1702.48	minimum of E_+
1310	2008	1703.52	1703.57	1703.46	minimum of E(I.S.)
1320	2410	1703.49	1703.50	1703.48	minimum of E_-

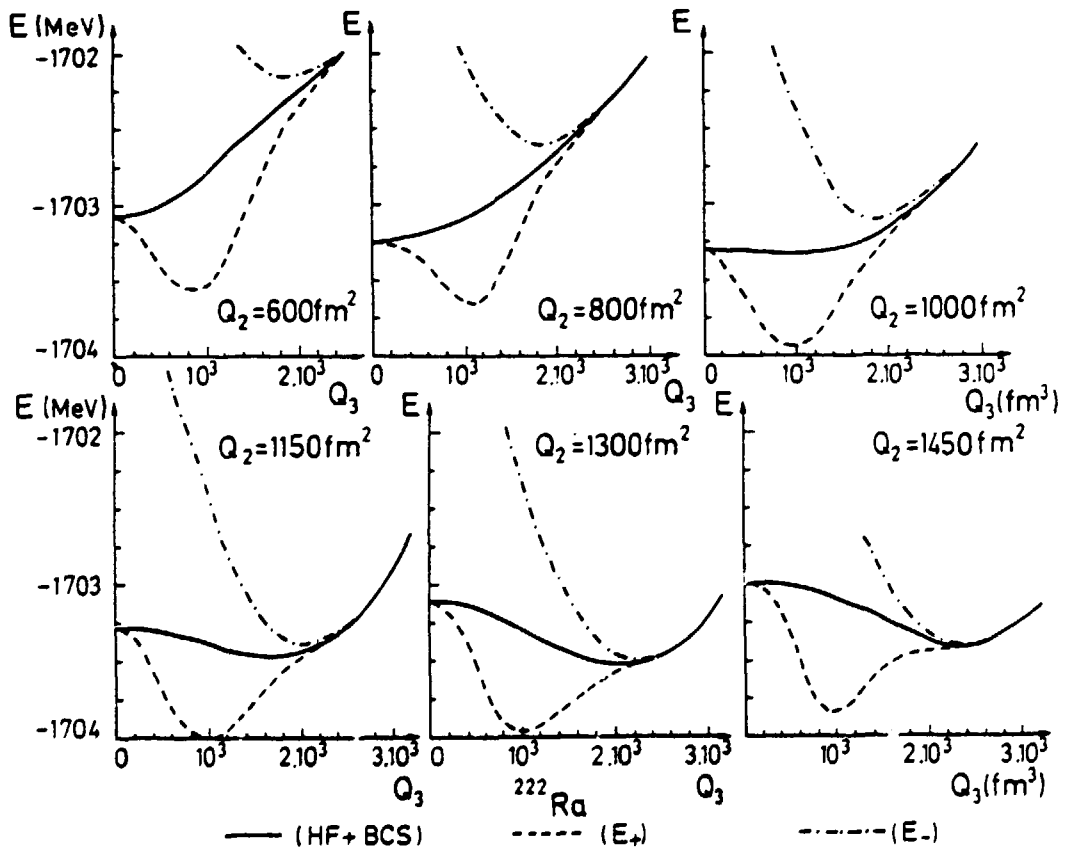


Figure 3. Energy curves for ^{222}Ra as a function of the octupole deformation Q_3 for several values of the quadrupole moment. The different lines represent the H.F. calculation of the unprojected state (HF+BCS), the positive parity state (E_+), and the negative parity state (E_-).

findings. The experimental 1^- state has an excitation energy of 0.24 Mev. The energy difference between the calculated intrinsic states (0.6 Mev) has the right order of magnitude although larger. A complete dynamical calculation by mean of the generator coordinate method for instance, may improve significantly the agreement.

The set of results we have obtained for this nucleus is shown on Fig. 3, where the minima listed in table 1 can be seen on the different curves. The absolute minimum of the negative state (E_-) is observed on the curves labeled $Q_2=1300 \text{ fm}^2$, it has a slightly larger value of Q_2 (1320 fm^2) as the response of a system to a constraint takes into account the restoring force: the system is driven to the minimum of the unprojected state. The other minima are deeper and numerically easier to get. These calculations have been performed for a value zero of the asymmetry angle. The γ -stability of these minima remains to be checked.

The $Z \sim 56$ isotopes have also been found to be good candidates for permanent octupole deformation in their ground states. Indeed, nuclear properties of neutron rich barium nuclei have been measured [20,21], and evidence for octupole bands in this mass region has been established experimentally [22]. Strutinsky-type potential-energy calculations [15,23] have shown that below $A \approx 200$, the nuclei $^{144,146}\text{Ba}$ are the best candidates for having a ground-state octupole deformation.

We have performed a similar calculation with the microscopic self-consistent H.F. method, choosing ^{144}Ba as a test case. Figure 4 shows that there is undoubtedly an octupole shell effect for this nucleus. With our present choice of the pairing strength, the intrinsic state is very soft with respect to octupole deformation, but the minimum in energy is obtained for $Q_2 \approx 500 \text{ fm}^2$ with $Q_3=0$. Within the uncertainties in the determination of the pairing strength, it is not possible to conclude whether or not a permanent octupole deformation is to be ruled out. However, when the intrinsic state is projected onto good-parity states, the minimum of the positive-parity band acquires an octupole deformation of 600 fm^3 for a quadrupole moment of 400 fm^2 . Our calculations do not extend to large enough quadrupole deformation so that we do not know the exact position of the minimum of the

negative-parity band. From the figure, we can only infer that it will have a much larger quadrupole moment: at least 800 fm^2 . In the upper part of Fig. 4 the overlap between the intrinsic state and the state obtained by parity reflection is given as a function of Q_3 . For extreme octupole deformation, this overlap goes to zero and the projected energies become equal to that of the intrinsic state. For $Q_3 = 0$, the energy splitting due to projection is maximum.

A further investigation of the quadrupole-octupole energy surface of this nucleus is necessary in particular for higher

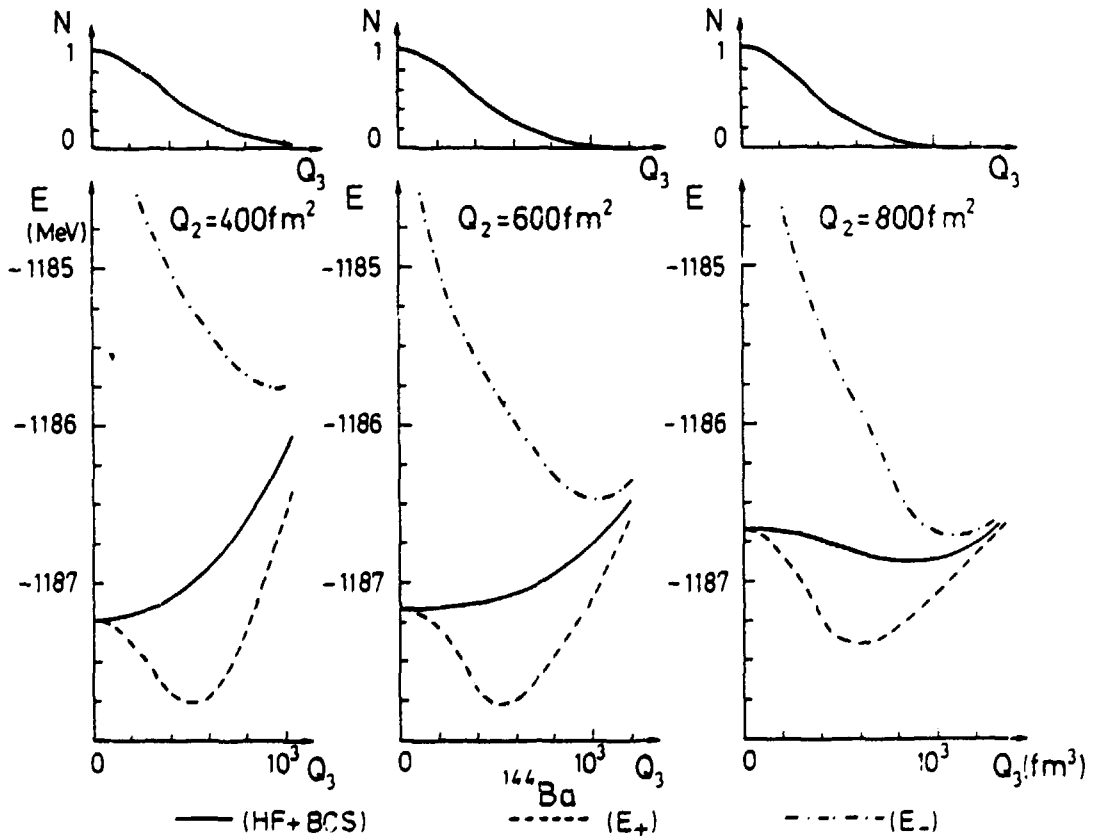


Figure 4. Energy of the intrinsic state (HF+BCS), the positive-parity state (E_+) and the negative-parity state (E_-) of the ^{144}Ba nucleus as a function of Q_3 for three values of the quadrupole moment. The upper part of the figure shows the overlap between the unprojected state and its parity reversed state.

quadrupole deformations. In addition we should pursue by the study of neighbouring isotopes such as ^{146}Ba or cerium isotopes in order to delineate the contour of the octupole deformation zone on the chart of elements. In the near future, we plan also to analyze the γ -stability of these shapes.

Finally, let us emphasize that we obtain for both nuclei a smaller quadrupole moment for the positive-parity band. From the first results, one can expect that this band will have a smaller moment of inertia, which seems to be the case for ^{222}Ra and ^{144}Ba [23].

SELF-CONSISTENT CRANKED HARTREE-FOCK

In this section, we present a generalisation of the discretized H.F. equations which incorporates rotations by mean of the cranked approximation. As a first application of this method we have studied the properties of a light nucleus, ^{24}Mg , from the ground state up to the fission limiting angular momentum [24].

The cranked approximation is based on the assumption that a nucleus with spin J can be described in terms of an intrinsic state at rest in a frame rotating with some angular velocity ω around a given axis. The optimal intrinsic state is determined by minimization of the Routhian \mathcal{E}

$$\mathcal{E} = E - \omega J_z, \quad (4)$$

where E is the expectation of the H.F. energy defined in eq. 1 and J_z the expectation value of the third moment of the angular momentum \hat{J}_z . The choice of the z -axis (contrary to the customary choice of the x -axis) simplifies the formulation of the symmetries of the single-particle wave-functions. As the cranked hamiltonian is no longer time-reversal invariant, the degeneracy of the single-particle wave functions does not hold anymore and we have to solve the cranked H.F. equations for each individual state, doubling therefore the size of the calculation. Furthermore, the structure of the mean-field is more

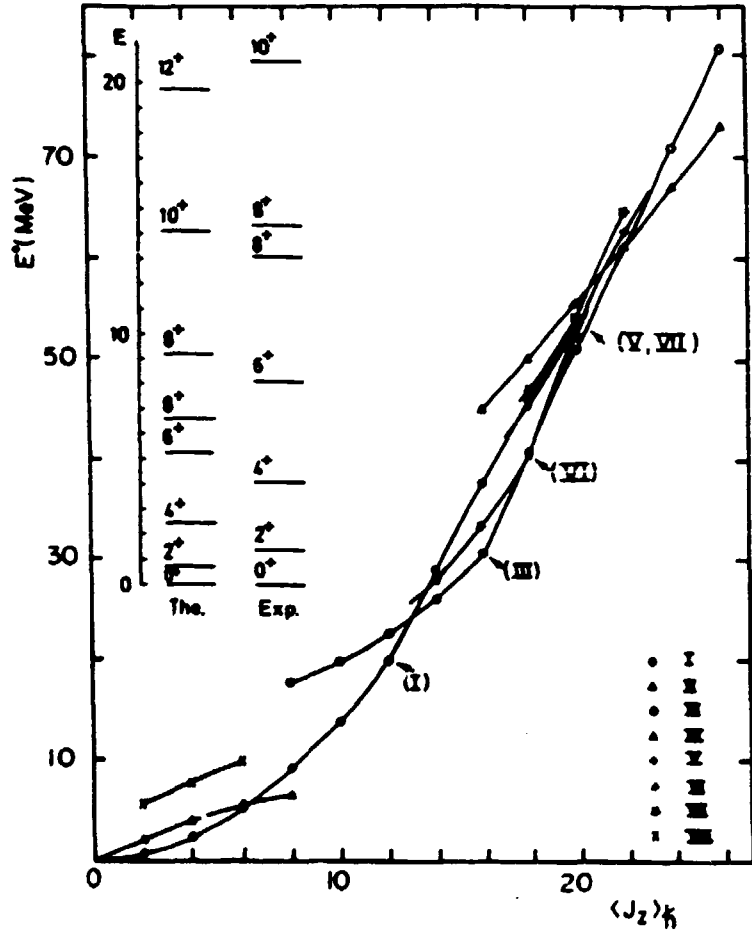


Figure 5. Excitation energy (in MeV) versus angular momentum (in \hbar) of various bands of ^{24}Mg . in the top left part of the figure is shown a comparison of the calculated and experimental spectra of the ground state band.

complicated, it includes spin-vector and current potentials which are usually neglected in semi-microscopic approaches.

For a nucleus as light as ^{24}Mg , pairing is not expected to play a significant role so that we use the simple BCS method. When time-reversal symmetry is broken, we follow the prescription proposed by Marshalek [25] to define paired states (see ref. 24 for a complete discussion of this approximation).

Low lying states of ^{24}Mg are known experimentally up to the Yrast 12^+ , and possibly 14^+ [26]. Strutinsky-type calculations have

been done for this nucleus [27,28]. Shell model calculations [29] are also available up to spin $J=12$.

The various bands generated by the rotation are displayed on Fig. 5. We will not elaborate on the details of these bands which have been adequately presented elsewhere [24]. Let us only recall the main differences with the Strutinsky-type calculation of ref. [28]. They find a triaxial ground state up to $J = 6$, as opposed to our prolate solution. Between $J = 6$ and 12, there results are very close to ours,

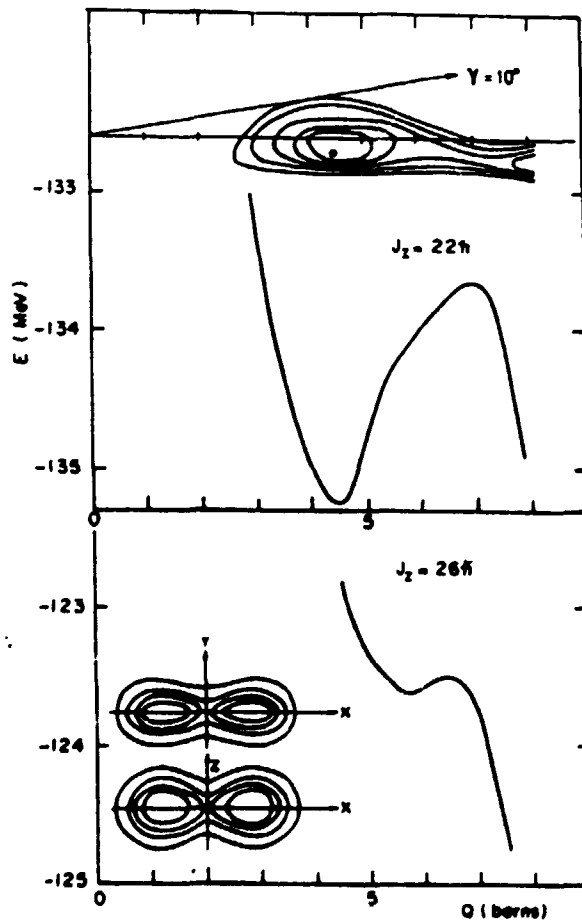


Figure 6. Fission path at $J = 22$ and 26 as a function of the quadrupole moment. The upper part shows the deformation energy curves at $J = 22$ (contour separated by 0.5 Mev). In the left-low corner are drawn two sections of the total density of the Yrast state at $J = 26$. The equidensity lines are drawn every 0.02fm^3 .

and in both cases, the spectrum is too compressed compared with experiment. In contrast with our calculation, their ground state band stops at $J = 12$. Above the ground state band and before fission, we have been able to extend some bands to lower spin (e.g. band II). There are other slight differences in the interpretation of the different bands which may be due to the absence of Y_4^2 and Y_4^4 components in the Nilsson-Strutinsky potential. As a matter of fact, most of the qualitative differences between their results and ours seem to come from the limitations of the parametrization of the potential shape in ref [28].

At the upper end of the Yrast line, from $J = 22$ to 26 on the band IV on fig. 5, the nucleus is quite elongated, ($400\text{fm}^2 < Q < 570\text{fm}^2$) and remains close to the prolate axis. For comparison, the end points of band III have quadrupole moments ranging from 80fm^2 to 100fm^2 (for $J = 24$). At the end of band IV, symmetric scission in two oblate ^{12}C occurs. The upper part of figure 6 gives the deformation energy surface for $(J_z) = 22$ with the corresponding fission path. The saddle point is slightly triaxial, however the energy dependence in γ is rather important as on the prolate axis ($\gamma = 0$), the energy is already 1.5 Mev above the saddle point ($\gamma = -4^\circ$). The lower part of the figure displays the fission path for the limiting angular momentum ($J = 26$). The density at the minimum is drawn in the left-low corner. The preformed ^{12}C are nearly oblate with their principal axes perpendicular to the rotation z-axis. This preformation can also be observed on the single-particle spectra where level are rearranging themselves in pairs of opposite parity [24]. The limiting angular momentum ($J = 26$) appears compatible with classical estimate [30].

CONCLUSION

Calculations of the deformation properties of the zirconium isotopes [2] have proven both the feasibility and the interest of the fully microscopic self-consistent Hartree-Fock approach when discretized in coordinate space. Exotic nuclei or triaxial shapes can be studied within its simplest version where states are time-reversal invariant and have no octupole deformation [8-11].

The study of octupole deformation presented in this talk [18] is already very interesting with the prediction of different moments of inertia for even and odd parity bands, however it remains incomplete as the γ -stability is yet to be investigated. We emphasize that this study will not require modifications of the present program which is clearly capable of describing both octupole and full quadrupole deformation (in fact all Y_{lm} deformations such that m is even). On the other hand, the projection code we have developed to extract good parity states opens the possibility of performing dynamical calculations. Projection is based on the estimation of matrix elements of the two-body hamiltonian between different Slater determinants, which is one of the ingredients required by the generator coordinate method. Such dynamical calculations are very promising for the study of fission for instance. Barriers for very asymmetric fission in the Ra-Th region could be obtained within such microscopic approach and compared with other semi-classical estimates.

The extension of H.F. to time-reversal non invariant states is by itself another field of interest. Besides the results presented above for ^{24}Mg [24], we have also analysed the influence of temperature on the behaviour of the Yrast line, which allows the study of high spin states with excitation energy or excited bands parallel to the Yrast line. With an improved treatment of the pairing interaction, we are presently investigating the high-spin properties of ^{80}Sr . Furthermore, the removal of time-reversal symmetry renders possible a microscopic study of odd-even or odd-odd nuclei without using artificially an even-even program (with time-reversal symmetry)

and ad-hoc partial filling of orbits. The exploration of the properties of odd exotic nuclei is thus possible microscopically, and remains to be done.

Finally, we are presently working on an extension of our program to include at the same time time-reversal non-invariant state and octupole deformation. Our goal is to analyse the structure of the odd and even bands in the Ba or the Ra-Th region as well as the high spin properties of these nuclei.

REFERENCES

1. See for instance S. Åberg, this conference and reference therein. see also Ref. 4, 5, 6, and 7 below.
2. P. Bonche, H. Flocard, P.H. Heenen, S.J. Krieger, M.S. Weiss, Nucl. Phys. A443 (1985) 39.
3. M. Girod and B. Grammaticos, Phys. Rev. C27 (1983) 2317.
4. P. Möller and J.R. Nix, At. Nucl. Tables 26 (1981) 165.
5. S. Åberg, Phys. Scripta 25 (1982) 23.
6. R. Bengtsson, P. Möller, J.R. Nix and Jing-Ye Zhang, Phys. Scripta 29 (1984) 1859.
7. I. Ragnarsson and R.K. Sheline, Phys. Scripta 29 (1984) 385.
8. A. Coc *et al.*, I.P.N. Orsay preprint, unpublished.
9. N. Redon *et al.*, Phys. Lett. B181 (1986) 223.
10. N. Redon *et al.*, 9^o Session d'Etudes biennale de Physique Nucléaire, Aussois, March 9-13 1987, France.
11. F. Naulin, Thèse d'Etat, Orsay (1987) France.
12. M. Uno and M. Yamada, Atomic mass prediction from the mass formula with empirical shell term. Ins. NUMA-40 (1982) Japan.
13. P. Möller, W.D. Myers, W.J. Swiatecki, J. Treiner, Los Alamos preprint (1986).
14. G.A. Leander, W. Nazarewicz, G.F. Bertsch, J. Dudek, Nucl. Phys. A453 (1986) 58.
15. W. Nazarewicz *et al.*, Nucl. Phys. A429 (1984) 269.
16. G.A. Leander, W. Nazarewicz, P. Olanders, I. Ragnarsson and J. Dudek, Phys. Lett. B152 (1985) 284.
17. C. Lederer and V. Shirley, Tables of isotopes (1978) J. Wiley and sons.
18. P. Bonche, P.H. Heenen, H. Flocard and D. Vautherin, Phys. Lett. B175 (1986) 387.
19. H.J. Rose and G.A. Jones, Nature 307 (1984) 245; S. Gales *et al.*, Phys. Rev. Lett. 53 (1984) 759; P.B. Price *et al.*, Phys. Rev. Lett. 54 (1985) 297; E. Hourani *et al.*, Phys. Lett. B106 (1985) 375.
20. C. Thibault *et al.*, Nucl. Phys. A367 (1981) 1.

21. S.M. Scott et al., J. of Phys. G6 (1980) 1291.
22. W.B. Walters et al., Proc. Int. Conf. on nuclei far from stability, Helsingør, CERN 81-09 (1981) 557.
23. W. Nazarewicz, private communication.
24. P. Bonche, H. Flocard and P.H. Heenen, Nucl. Phys. A467 (1987) 115.
25. E. Marshalek, Phys. Rev. C15 (1977) 1574.
26. Y. Horikawa et al., Phys. Lett. B36 (1971) 9; E.W. Lees et al., J. of Phys. G2 (1976) 105; M.P. Fewell et al., Nucl. Phys. A319 (1979) 214; S.A. Wender et al., Phys. Rev. C17 (1978) 1365; J.L.C. Ford jr. et al., Phys. Rev. C21 (1980) 764; A. Szanto de Toledo et al., Phys. Rev. C30 (1984) 706.
27. M. Diebel, D. Glas, U. Mosel and H. Chandra, Nucl. Phys. A333 (1980) 253.
28. I. Ragnarsson, S. Åberg and R. Sheline, Phys. Scr. 24 (1981) 215.
29. A. Watt, D. Kelvin and R.R. Whitehead, Phys Lett. B63 (1979) 385.
30. S. Cohen, F. Plasil and W.J. Swiatecki, Ann. Phys. 82 (1974) 557.